H-Spillover through the Catalyst Saturation: An *Ab Initio* Thermodynamics Study

Abhishek K. Singh, Morgana A. Ribas, and Boris I. Yakobson*

Department of Mechanical Engineering and Materials Science, Department of Chemistry, and The Richard E. Smalley Institute for Nanoscale Science and Technology, Rice University, Houston, Texas 77005

Hydrogen is a carrier of clean energy[1,2] and can be easily generated from renewable sources. A cost-effective, safe, and efficient storage medium is the key to utilize its full potential. Among the various possibilities, the carbon-based adsorbents[3−8] are recognized as strong candidates, where large surface area and lighter weight make the substantial volumetric and gravimetric content possible. Furthermore, the storage capacity of graphitic materials (*e.g.*, nanotubes and fullerenes) can be significantly enhanced by decorating them with metal atoms,[9−14] which absorb multiple H_2 molecules *via* Kubas interaction.[15] Although promising, the experimental efforts in synthesizing the metal-decorated nanotubes and fullerenes have not been successful so far. Additionally, the tendency of metal atoms to cluster[16,17] leads to considerable reduction in potential storage capacity. In contrast, the metal cluster supported on graphitic materials acts as a catalyst and enhances the hydrogen uptake of substrates *via* spillover.[18−21]

The spillover process involves the transport of an active species (*e.g.*, H) formed on a catalyst onto a receptor that does not sorb the species[22] under the same conditions. Current growing interest in efficient storage of hydrogen brought this long-known phenomenon into the spotlight. The most widely used catalysts for spillover of H atoms on graphitic materials are Ni, Pd, Pt, and other transition metal atoms. Recently, several experiments have shown the enhancement of H_2 adsorption *via* spillover on activated carbons and MOF.[19,23−25] Up to 4 wt % of adsorption has been reported for IRMOF-8 at 298 K and 10 MPa.[26] Furthermore, it is empirically established that the spillover can be enhanced by adding so-

ABSTRACT The spillover phenomenon, which essentially involves transfer of H from a metal catalyst to a graphitic receptor, has been considered promising for efficient hydrogen storage. An open question about the spillover mechanism is how a H atom binds to graphene instead of forming the thermodynamically preferred H_2. Using *ab initio* calculations, we show that the catalyst saturation provides a way to the adsorption of hydrogen on the receptor by increasing the H chemical potential to a spillover favorable range. Although it is energetically unfavorable for the spillover to occur on a pristine graphene surface, presence of a phase of hydrogenated graphene facilitates the spillover by significantly improving the C−H binding. We show that thermodynamic spillover can occur, both from the free-standing and from the receptor-supported clusters. Further, the computed energy barrier of the motion of a H from the catalyst to the hydrogenated graphene is small (0.7 eV) and can be overcome at operational temperatures.

KEYWORDS: hydrogen storage · spillover · catalysis · graphene · *ab initio* thermodynamics

called bridges[24] between the catalyst and receptor. Although exact distribution and the binding sites of the H remain experimentally unspecified, it is reasonable to suggest that the best coverage of the H on graphitic substrates can be achieved when they are hydrogenated on both sides,[27,28] and spillover is considered as a possible path to achieving it. Thus, fully hydrogenated graphene would have stoichiometry CH, with 7.7 wt % of hydrogen,[27−30] meeting the DOE goals. Even though the spillover of the H on graphitic surfaces was observed decades ago,[22] it is still not well-understood how a H binds to graphene when it seems energetically more favorable to stay on the catalyst or even to remain in a molecular H_2 form in the gas phase. To better understand the spillover mechanism, with the goal to optimize its kinetics, it is important to compare the relative energy states of the hydrogen in its (i) dihydrogen gas form, (ii) at the metal catalyst, and (iii) on the receptor substrate (Figure 1). The energy states available for H will depend on the degree of saturation or substrate coverage.

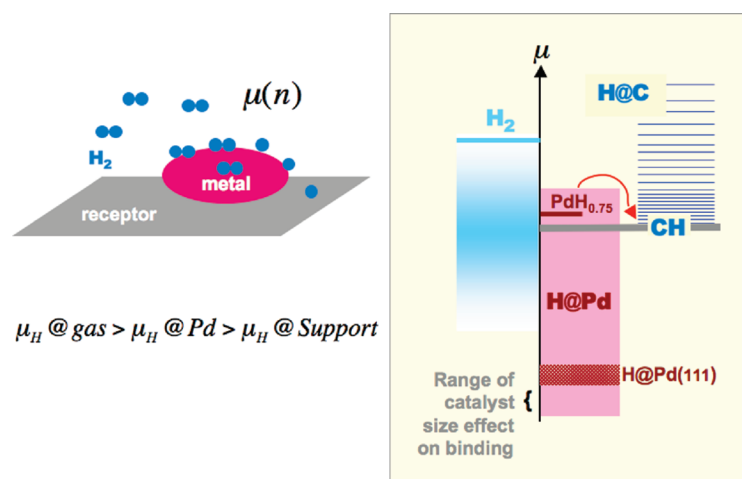*Address correspondence to
biy@rice.edu.

Figure 1. Left: Schematics of spillover process in real space. The inequality shows the range of chemical potential μ_H favorable for spillover. Right: model of spillover in energy space displays the relative energy (chemical potential) of H in different states. The gray, dark-red, and blue lines show the μ_H in fully hydrogenated graphene (CH), in metal hydride (PdH$_{0.75}$), and in the H$_2$ molecule, respectively. The pink and dark-red blocks show the range of energies of H at the catalyst and at the Pd(111) surface with the H coverage varying form 0.25 to 1 ML. The family of thin dark-blue lines corresponds to the energies of H bound to graphene.

Indeed, Cheng *et al.* have studied[31,32] the dissociative chemisorption of molecular hydrogen and desorption of atomic hydrogen on Pt clusters and concluded that the number of adsorbed H$_2$ increases with the increasing size of the cluster. Furthermore, they show that the binding strengths *decrease* with the increasing coverage, that is, energy states available for H raise, approximately representing the increase of the chemical potential μ_H since the entropy contribution is less significant. They find that in low coverage the adsorption strengths are very large and at the saturation level are closer to the energies on a fully H-covered Pt(111) surface.[31,32] In contrast, the strength of a H binding to sp^2-carbon receptor is shown to *increase* with the greater coverage, due to its clustering and CH phase formation.[30] This analysis reconciles the fact of spillover with too weak binding of the H to the bare substrate, by stressing the role of nucleation of *condensed* CH phase, which must be forming in the process of spillover on a graphene receptor, as it is more favorable than a H$_2$ molecule.[30] In our previous study, the catalyst *per se* was not considered, and the focus was on the variation of the hydrogen binding to the receptor and its thermodynamic comparison with gaseous H$_2$.

Here we report the details of hydrogen binding to the catalyst particle, which serves as a gateway to the entire process and whose saturation is also an important aspect of spillover. Combining molecular dihydrogen gas phase, H dissolved on the catalyst, and H in the "storage phase" on the receptor, a conceptual quantitative diagram of spillover is drawn in Figure 1. On the left, the blue line marks the energy of H in its molecular form and the additional broad (also blue) range is the chemical potential of H including the entropic con-

tribution at different gas conditions. On the right side, a family of thin dark-blue lines corresponds to the energies of H bound to graphene, which vary with the size and the configuration of the cluster island[30] and converge to the CH phase energy. The midsection pink block shows the range of energies of H at the catalyst as computed and analyzed below. The first H$_2$ molecule dissociates and binds to the catalyst rather strongly; and therefore, μ_H lies deep in this picture. However, the energies of the subsequent H$_2$ binding gradually decrease, raising the μ_H. For the spillover of a H to occur from the metal, the μ_H must exceed the CH state energy level shown by the gray line, before the metal cluster saturates (*i.e.*, becomes unable to further accept new H$_2$ molecules). The catalyst plays an important role in bringing the μ_H into this range. Possible metal-hydride phase formation imposes an additional constraint on the μ_H. The former must lie above the μ_H of the receptor to avoid formation of metal-hydride before the spillover (assuming that the hydride phase would inhibit the catalytic activity). In this work, we validate this model by exploring through *ab initio* computations the gradual energy change of H on the catalyst to reveal how it fits between the energy on the receptor and as free gas. Comparing these μ_H values identifies the range of chemical potential favorable for the spillover. The role of catalyst saturation and binding strength of H with the receptor in bringing the μ_H in this desirable range is explored. Furthermore, to understand the first kinetic step, the barrier involved in the motion of a H atom from catalyst to receptor is computed and compared with the experimental observation.

RESULTS AND DISCUSSION

In order to get the μ_H on the metal catalyst, hydrogen uptake process of a free *unsupported* cluster was performed. More specifically, we consider relatively small four-atom Ni and Pd clusters as catalysts and a graphene with the H-terminated edge as receptor. The binding energy as well as the chemical potential of H$_2$ on the metal cluster will depend upon the number of H$_2$ attached and the relative positions of the H atoms. For example, the binding energy of the first H$_2$ on the cluster will differ from the next H$_2$ and so on. Addition of a H$_2$ molecule leads to gain in the incremental energy, which approximately represents the chemical potential μ_H, which is defined as

$$\mu_H = \Delta E(M_nH_m) = [E(M_nH_m) - E(H_2) - E(M_nH_{m-2})]/2$$

where M$_n$ is a metal catalyst. A comparison of the $\mu_H(m)$ in the metal cluster and in the receptor provides the number of H$_2$ molecules required to saturate the metal cluster sufficiently to permit the spillover onto the receptor.

The geometries of the Pd_4 cluster are optimized, and among the various structures, a tetrahedron is found to be the lowest in energy.[33] The magnetic moment (2 μ_B) and the Pd−Pd bond lengths (2.65 Å) in the Pd_4 cluster are in good agreement with the previous calculations[33] performed by using the hybrid B3LYP exchange correlation functional, which gives a better description of the transition metals. The comparison provides an independent test of the method accuracy. For the subsequent hydrogenation of the catalyst, several symmetrically nonequivalent adsorption sites for a H_2 molecule on the cluster are considered, and their respective energies are compared. The first H_2 dissociatively adsorbs on the Pd_4 cluster (essentially forming a hydride molecule). Among the various structures of the Pd_4H_2, there are two lowest energy configurations, as was observed in the previous calculation.[33] In one of the structures, the dissociated H atoms cap the adjacent triangular faces of the Pd_4 cluster (Figure 2a), while in the other, they bridge the Pd−Pd edges, which do not have the common Pd atom. We continued hydrogenation by subsequently adding the H_2 molecules to the ground state structure (cluster + H_2) obtained from the previous optimization. From the second H_2 onward, H_2 molecules do not fully dissociate, but rather bind to Pd_4 via Kubas[15] type of interaction, where the H−H bonds are elongated from 0.73 Å (as in molecular H_2) to 0.84−0.87 Å. The hydrogenation was continued until the cluster stopped to adsorb any further H_2, that is, no bound stable configuration could be found. The Pd_4 cluster saturates after adsorbing nine H_2 molecules. The optimized geometries of these clusters are shown in Figure 2a. The 10th H_2 is repelled from the cluster and remains in the molecular form. This unattached H_2 lies more than 3.3 Å away from the atoms of the saturated cluster. The H−H bond length remains the same as in the molecular H_2, accompanied by almost no gain in binding energy, signaling the saturation of the cluster.

The incremental energies ΔE, which are plotted in Figure 2b, never exceed the energy of a H on a pristine graphene (not shown in Figure 2, and corresponding to the topmost thin line on the right side of Figure 1). Hence, thermodynamically spillover cannot be easily initiated on a pristine graphene. The possibility cannot be completely excluded because at higher temperature due to fluctuations some of the H atoms can move to the graphene. On the other hand, the incremental binding energies do exceed the chemical potential of H in the hydrogenated phase, after the adsorption of the sixth H_2 molecule, as shown in Figure 2b (the gray line there corresponds to the thin gray line in Figure 1, as well). Therefore, the spillover to the fully hydrogenated phase is indeed thermodynamically favorable after the catalyst has adsorbed six H_2 molecules.
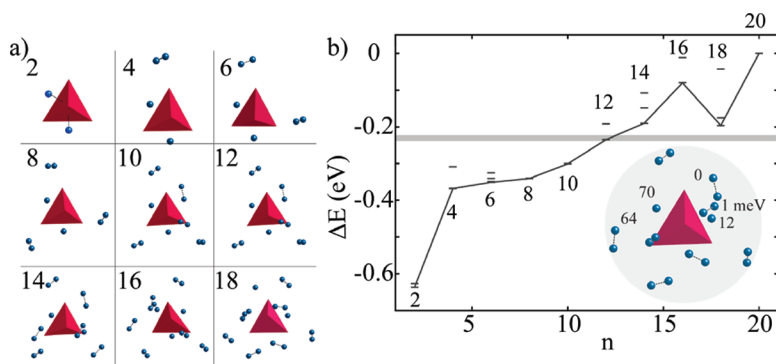

Figure 2. (a) Optimized structures of Pd_4H_n ($n = 2−18$) clusters. (b) Plot of ΔE with the increasing number of H atoms. The gray dashes are the energies of other isomers. The horizontal gray line shows the μ_H in a fully hydrogenated graphene. Inset: optimized geometry of a fully saturated Pd_4H_{18} cluster. The energies are given with respect to the energy (0) of the most stable H.

Due to computational limitations, we use a small cluster to model the catalyst, but the qualitative conclusions on spillover are quite general. Although we believe that the overall chemisorption behavior of catalyst does not change much with increasing size,[31] some additional complications may appear. Among them could be possible bulk metal-hydride phase formation. In order to assess this, we have separately calculated chemical potential of H in the Pd-hydride crystal ($PdH_{0.75}$) using standard periodic boundary conditions instead of cluster approach. The result is shown in Figure 1 by the red line, which lies ~60 meV above the gray CH line. Hence, in the case of Pd, the spillover will occur before formation of hydride. The position of this line may vary for different metal catalysts, which is helpful in determining the best metal catalyst for spillover and could be further tuned/optimized by alloying. We also calculate the adsorption energy of the H on Pd(111) surface for coverage from 0.25 to 1 ML, shown by the red block in Figure 1. The adsorption energy of 0.25 ML hydrogen is 0.57 eV, only slightly higher (~0.1 eV) than that in the Pd_4. Hence, with increasing cluster size, the threshold of the spillover may decrease but not very significantly.

Additionally, in order to study the effect of different metal element catalysts on the spillover, we also carried out simulated hydrogenation of a Ni_4 cluster. The ground state geometry of the Ni_4 is found to be a tetrahedron, with the Ni−Ni bond length of 2.60 Å and magnetic moment of 4 μ_B. The larger magnetic moment arises due to localized nature of the Ni 3d orbital. The Ni_4 adsorbs the first two H_2 molecules dissociatively. The cluster saturates after adsorbing the 10th H_2 molecule. The incremental binding energy exceeds the chemical potential of H in hydrogenated phase, after the adsorption of the seventh H_2 (Figure S1 in Supporting Information). Therefore, the effect of changing the metal from Pd to Ni essentially shifts the threshold of the spillover from sixth to seventh H_2 because of the more diffused nature of Pd 4d orbital compared with the Ni 3d orbital.
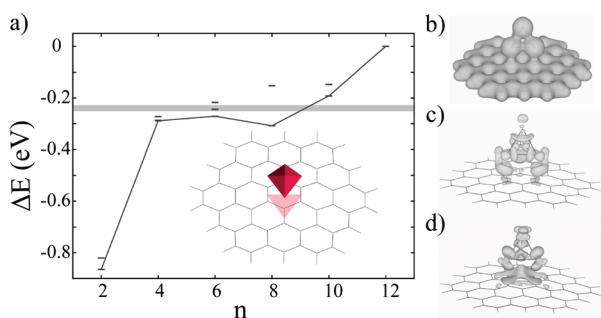
Figure 3. (a) Plot of incremental energy Δ*E versus* number of H atoms on supported cluster. Gray dashes are the energies of other isomers. Inset: optimized geometry of Pd$_4$@graphene. The gray line shows the μ_H in a fully hydrogenated graphene. (b−d) Isosurfaces of the total, accumulation, and depletion of charges.

The overall trend in the hydrogenation of the Ni$_4$ cluster remains similar to the Pd$_4$ (Figure S1 in Supporting Information); therefore, further analysis is carried out only on the Pd$_4$ cluster.

The justification of considering incremental energies as chemical potential (essentially an average quantity) depends on how large the variance is in the removal energies of the different H atoms from a saturated cluster/catalyst. The energy cost to remove a H from the cluster may, in principle, differ with the type/position of the removed atom. In order to evaluate this, we have calculated the removal energies of the five symmetrically nonequivalent H atoms including Kubas and dissociated from fully saturated Pd$_4$H$_{18}$ as shown in Figure 2b, inset. The difference in removal energies of the five nonequivalent atoms lies within 70 meV, which is relatively small. This energy difference is within 15% of the total range of chemical potential of H on a catalyst and is reasonable enough to justify its use as a chemical potential. This difference is expected to decrease with the increasing size of the catalyst. Moreover, the bonding strengths of the Kubas type H atoms are similar to the dissociatively adsorbed H atoms, indicating that any atom could potentially participate in the spillover process as long as μ_H of the system has reached high enough level at overall saturation.

The above analysis shows that it is energetically possible for spillover to occur from an unsupported metal cluster to a receptor. In experiments, these clusters are supported on the substrate, and hydrogen diffuses (or rather hops) from the catalyst to the support/receptor.[34] In order to make our model closer to the experimental situation, we next studied the hydrogenation of a *supported* cluster on a receptor. The pristine graphene was chosen as support as the C atoms in the vicinity of the catalyst might exhibit improved binding with the hydrogen. First, several nonequivalent sites for Pd$_4$ cluster on graphene have been optimized. After relaxation, however, most of the configurations converge to a structure, where three corners of the tetrahedron lie above the centers of C−C bonds (Figure 3). There are two types of Pd−Pd bond with the bond lengths of

2.60 and 2.69 Å, whereas average Pd−C bond lengths are 2.30 Å. The binding energy and the total magnetic moment of the whole Pd$_4$ cluster on the graphene are 0.42 eV and 1 μ_B (reduced from the unsupported cluster), respectively.

The bonding of receptor and catalyst is analyzed by plotting the total, accumulation, and depletion of charges, shown in Figure 3b−d, respectively. The accumulation/depletion of charges is obtained by subtracting the total charges of free Pd$_4$ cluster and graphene calculated independently, with the same atomic position, from the total charge of the Pd$_4$@graphene. The positive (negative) value of the isosurface represents the accumulated (depleted) charge regions. The total charge density shows some directionality of the C−Pd bond; nevertheless, the charges around Pd are diffused, a signature of a mixed covalent and metallic bonding (Figure 3b). Further evidence comes from the isosurfaces of accumulation and depletion, as the charge has been accumulated between the C−Pd bonds and depleted from the π-cloud of hexagonal ring in graphene (Figure 3c,d).

Next, the hydrogenation of this supported cluster was performed, following the same procedure as described above for the free cluster. Like on the free cluster, the first H$_2$ is adsorbed dissociatively, and subsequent ones bind *via* Kubas interaction.[15] The cluster saturates with five H$_2$ molecules, much sooner than the free cluster. As expected, the incremental adsorption energy never exceeds the energy of a H on pristine graphene. However, it does cross the level line of C−H energy of a fully hydrogenated graphene after the adsorption of the fifth H$_2$ molecule, hence showing the thermodynamic possibility of the spillover. The onset of spillover occurs earlier than in the free cluster because the charge available for binding with the H$_2$ is now shared with the support material. This reduces the overall intake of H on the catalyst, with no harm to spillover.

Having shown the possibility of the spillover from both free and supported cluster, we turn to the kinetics aspects, which essentially involve the motion of the H atom from the metal to the receptor. The likelihood of a H atom to hop from the catalyst to the pristine graphene substrate was tested in a computational experiment by removing the H atom from the saturated catalyst and bringing it to the receptor. Upon relaxation, H goes back to the catalyst spontaneously. When the removed hydrogen is placed farther away from the catalyst, it remains attached but the whole process is rather endothermic, highlighting again the difficulty of spillover on pristine graphene. Similarly, we tested a H atom hopping to the receptor in the vicinity of a fully hydrogenated graphene phase, which was represented by hydrogenated ring hexagon near the catalyst. In this case, the H atom removed from the catalyst is more stable on the hydrogenated phase: unlike in the pris-

tine graphene case, the H does not come back to the catalyst, and the overall process becomes energetically favorable by 0.15 eV, making spillover possible on hydrogenated graphene.[34]

Although it is more favorable for H to be in the hydrogenated phase than on the saturated catalyst, there are still barriers involved for the motion of the H. The migration barrier for H to move from the metal to CH phase is calculated using nudged elastic band method[36] (Figure 4). The barrier is $E_s = 0.68$ eV, which can be overcome even below the room temperature. Indeed, at $k_BT = 0.025$ eV, the characteristic time τ of this step can be estimated from standard rate theory[37] as $\tau^{-1} = (k_BT/h) \cdot \exp(-E_s/k_BT)$. With the prefactor $k_BT/h = 10^{13}$ s^{-1}, one obtains $\tau \approx 30$ ms—a reasonably fast stage.[34] Therefore, spillover is both thermodynamically favorable and kinetically feasible under the ambient conditions.

CONCLUSIONS

In summary, we have shown the thermodynamic and kinetic plausibility of the spillover process. Energetically, it is possible for spillover of H to occur from a metal cluster to the hydrogenated graphene, both from the free-standing and from the receptor-supported clusters. Importantly, the process does not require full saturation of the cluster because thermodynamic spillover becomes favorable even before a cluster saturates. Furthermore, it is energetically unfavorable for the spillover to occur on pristine graphene surfaces, yet a phase of hydrogenated graphene facilitates the process by significantly improving the C−H binding. The migra-
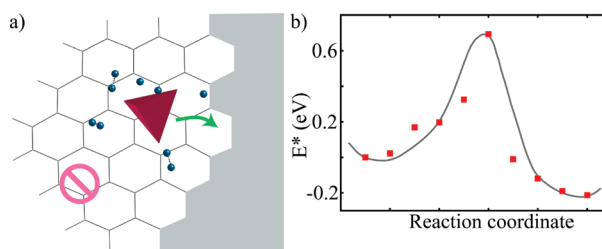

Figure 4. (a) Fully relaxed cluster saturated with H, next to hydrogenated phase (gray area). (b) Plot of energies of intermediate images for the barrier calculation *versus* the reaction coordinate.

tion barrier for hydrogen from the metal cluster to the hydrogenated phase is small, suggesting that the spillover can easily occur below room temperature. These findings are in agreement with the recent experiments, where H uptake *via* the spillover increases with the temperature and the reduction of the substrate.[38] Moreover, this work provides possibly the first explanation of the "nano-thermodynamics" of spillover and also hints toward finding materials where it can be achieved more effectively. Along with the catalyst saturation, the optimum C−H bonding has emerged as an important factor for the spillover. Therefore, any modification of the receptor that leads to an increase in this energy will also enhance the spillover (of course, within the reversibility limits). The incorporation of defects, curvature, and dopants is a few of the potential routes to facilitate nucleation by improving the C−H binding. For example, this has been demonstrated for graphene where the energy of hydrogenation changes drastically by Stone−Wales types of defects.[39]

METHODS

The calculations are based on the density functional method with all-electron projected augmented wave potentials[40,41] and the generalized gradient approximation of the Perdew−Burke−Ernzerhof (PBE)[42] for exchange and correlation, as implemented in VASP.[43,44] Gamma point is used for Brillouin zone sampling. Conjugate gradient scheme is employed to relax the geometry until the forces on every atom are less than 0.005 eV/Å. Large vacuum spaces (∼15 Å) are used in supercells to minimize any cell−cell spurious interactions. The migration barrier for a H atom is calculated using nudged elastic band method.[36]

Supporting Information Available: Figure S1. This material is available free of charge *via* the Internet at http://pubs.acs.org.

REFERENCES AND NOTES

1. Crabtree, G. W.; Dresselhaus, M. S.; Buchanan, M. V. The Hydrogen Economy. *Phys. Today* **2004**, 39–44.

2. Schlapbach, L.; Züttel, A. Hydrogen-Storage Materials for Mobile Applications. *Nature* **2001**, *414*, 353–358.

3. Dillon, A. C.; Jones, K. M.; Bekkedahl, T. A.; Kiang, C. H.; Bethune, D. S.; Heben, M. J. Storage of Hydrogen in Single-Walled Carbon Nanotubes. *Nature* **1997**, *386*, 377–379.

4. Ding, F.; Lin, Y.; Krasnov, P. O.; Yakobson, B. I. Nanotube-Derived Carbon Foam for Hydrogen Sorption. *J. Chem. Phys.* **2007**, *127*, 164703-1–164703-6.

5. Ye, Y.; Ahn, C. C.; Witham, C.; Fultza, B.; Liu, J.; Rinzler, A. G.; Colbert, D.; Smith, K. A.; Smalley, R. E. Hydrogen Adsorption and Cohesive Energy of Single-Walled Carbon Nanotubes. *Appl. Phys. Lett.* **1999**, *74*, 2307–2309.

6. Liu, C.; Fan, Y. Y.; Liu, M.; Cong, H. T.; Cheng, H. M.; Dresselhaus, M. S. Nanotubes at Room Temperature Hydrogen Storage in Single-Walled Carbon. *Science* **1999**, *286*, 1127–1129.

7. Yoon, M.; Yang, S.; Wang, E.; Zhang, Z. Charged Fullerenes as High-Capacity Hydrogen Storage Media. *Nano Lett.* **2007**, *7*, 2578–2583.

8. Pupysheva, O. V.; Farajian, A. A.; Yakobson, B. I. Fullerene Nanocage Capacity for Hydrogen Storage. *Nano Lett.* **2008**, *8*, 767–774.

9. Kiran, B.; Kandalam, A. K.; Jena, P. Hydrogen Storage and the 18-Electron Rule. *J. Chem. Phys.* **2006**, *124*, 224703-1–224703-6.

10. Durgun, E.; Jang, Y.-R.; Ciraci, S. Hydrogen Storage Capacity of Ti-Doped Boron-Nitride and B/Be-Substituted Carbon Nanotubes. *Phys Rev. B* **2007**, *76*, 073413-1–073413-4.

11. Zhao, Y.; Kim, Y.-H.; Dillon, A. C.; Heben, M. J.; Zhang, S. B. Hydrogen Storage in Novel Organometallic Buckyballs. *Phys. Rev. Lett.* **2005**, *94*, 155504-1–155504-4.

12. Phillips, A. B.; Shivaram, B. S. High Capacity Hydrogen Absorption in Transition Metal-Ethylene Complexes Observed *via* Nanogravimetry. *Phys. Rev. Lett.* **2008**, *100*, 105505-1–105505-4.

13. Yildirim, T.; Ciraci, S. Titanium-Decorated Carbon Nanotubes as a Potential High-Capacity Hydrogen Storage Medium. *Phys. Rev. Lett.* **2005**, *94*, 175501-1–175501-4.

14. Yildirim, T.; Iñiguez, J.; Ciraci, S. Molecular and Dissociative Adsorption of Multiple Hydrogen Molecules on Transition Metal Decorated C_{60}. *Phys Rev. B* **2005**, *72*, 153403-1–153403-4.

15. Kubas, G. J. Molecular Hydrogen Complexes: Coordination of a CT Bond to Transition Metals. *Acc. Chem. Res.* **1988**, *21*, 120–128.

16. Sun, Q.; Wang, Q.; Jena, P.; Kawazoe, Y. Clustering of Ti on a C_{60} Surface and Its Effect on Hydrogen Storage. *J. Am. Chem. Soc.* **2005**, *127*, 14582–14583.

17. Krasnov, P. O.; Ding, F.; Singh, A. K.; Yakobson, B. I. Clustering of Sc on SWNT and Reduction of Hydrogen Uptake: *Ab-Initio* All-Electron Calculations. *J. Phys. Chem. C* **2007**, *111*, 17977–17980.

18. Lueking, A. D.; Yang, R. T. Hydrogen Spillover to Enhance Hydrogen Storage Study of the Effect of Carbon Physicochemical Properties. *Appl. Catal., A* **2004**, *265*, 259–268.

19. Li, Y.; Yang, R. T. Significantly Enhanced Hydrogen Storage in Metal-Organic Frameworks *via* Spillover. *J. Am. Chem. Soc.* **2005**, *128*, 726–727.

20. Zacharia, R.; Kim, K. Y.; Kibria, A. K. M. F.; Nahm, K. S. Enhancement of Hydrogen Storage Capacity of Carbon Nanotubes *via* Spill-over from Vanadium and Palladium Nanoparticles. *Chem. Phys. Lett.* **2005**, *412*, 369–375.

21. Kim, B.-J.; Lee, Y.-S.; Park, S.-J. Preparation of Platinum-Decorated Porous Graphite Nanofibers, and Their Hydrogen Storage Behaviors. *J. Colloid Interface Sci.* **2008**, *318*, 530–533.

22. Conner, W. C.; Pajonk, G. M.; Teichner, S. J. *Spillover of Sorbed Species*; Academic Press: Orlando, FL, 1986; Vol. 34, p 1.

23. Liu, Y.-Y.; Zeng, J.-L.; Zhang, J.; Xu, F.; Sun, L.-X. Improved Hydrogen Storage in the Modified Metal-Organic Frameworks by Hydrogen Spillover Effect. *Int. J. Hydrogen Energy* **2007**, *32*, 4005–4010.

24. Lachawiec, A. J., Jr; Qi, G.; Yang, R. T. Hydrogen Storage in Nanostructured Carbons by Spillover: Bridge-Building Enhancement. *Langmuir* **2005**, *21*, 11418–11424.

25. Bourlinos, A.; Kouvelos, E.; Miller, M. A.; Zlotea, C.; Stubos, A.; Steriotis, T. Submitted.

26. Li, Y.; Yang, R. T. Hydrogen Storage in Metal-Organic Frameworks by Bridged Hydrogen Spillover. *J. Am. Chem. Soc.* **2006**, *128*, 8136–8137.

27. Lueking, A. D.; Gutierrez, H. R.; Fonseca, D. A.; Narayanan, D. L.; VanEssendelft, D.; Jain, P.; Clifford, C. E. B. Combined Hydrogen Production and Storage with Subsequent Carbon Crystallization. *J. Am. Chem. Soc.* **2006**, *128*, 7758–7760.

28. Sofo, J.; Chaudhari, A.; Barber, G. Graphane: A Two-Dimensional Hydrocarbon. *Phys. Rev. B* **2007**, *75*, 153401-1–153401-4.

29. Stojkovic, D.; Zhang, P.; Lammert, P.; Crespi, V. Collective Stabilization of Hydrogen Chemisorption on Graphenic Surfaces. *Phys. Rev. B* **2003**, *68*, 195406-1–195406-5.

30. Lin, Y.; Ding, F.; Yakobson, B. I. *Phys. Rev. B* **2008**, *78* 041402(R)-1–041402(R)-4.

31. Zhou, C.; Wu, J.; Nie, A.; Forrey, R. C.; Tachibana, A.; Cheng, H. On the Sequential Hydrogen Dissociative Chemisorption on Small Platinum Clusters: A Density Functional Theory Study. *J. Phys. Chem. C* **2007**, *111*, 12773–12778.

32. Chen, L.; Cooper, A. C.; Pez, G. P.; Cheng, H. Density Functional Study of Sequential H_2 Dissociative Chemisorption on a Pt_6 Cluster. *J. Phys. Chem. C* **2007**, *111*, 5514–5519.

33. Moc, J.; Musaev, D. G.; Morokuma, K. Adsorption of Multiple H_2 Molecules on Pd_3 and Pd_4 Clusters. A Density Functional Study. *J. Phys. Chem. A* **2000**, *104*, 11606–11614.

34. Our focus here is only the very first step—a diffusion hop from the catalyst to receptor. This of course must be followed by H diffusion on carbon sites away from metal, which has been demonstrated to be reasonably fast.[35]

35. Sha, X.; Knippenberg, M. T.; Cooper, A. C.; Pez, G. P.; Cheng, H. Dynamics of Hydrogen Spillover on Carbon-Based Materials. *J. Phys. Chem. C* **2008**, *112*, 17465–17470.

36. Jónsson, H.; Mills, G.; Jacobsen, K. W. *Nudged Elastic Band Method for Finding Minimum Energy Paths of Transitions*; World Scientific: River Edge, NJ, 1998; p 385.

37. Glasstone, S.; Laidler, K. J.; Eyring, H. *The Theory of Rate Processes*; McGraw-Hill Book Co: New York, 1941.

38. Wang, L.; Yang, R. T. Hydrogen Storage Properties of Carbons Doped with Ruthenium, Platinum, and Nickel Nanoparticles. *J. Phys. Chem. C* **2008**, *112*, 12486–12494.

39. Duplock, E. J; Scheffler, M.; Linda, P. J. D. Hallmark of Perfect Graphene. *Phys. Rev. Lett.* **2004**, *92*, 225502-1–225502-4.

40. Blöchl, P. E. Projector Augmented-Wave Method. *Phys. Rev. B* **1994**, *50*, 17953–17979.

41. Kresse, G.; Joubert, D. From Ultrasoft Pseudopotentials to the Projector Augmented-Wave Method. *Phys. Rev. B* **1999**, *59*, 1758–1775.

42. Perdew, J. P.; Burke, K.; Ernzerhof, M. Generalized Gradient Approximation Made Simple. *Phys. Rev. Lett.* **1996**, *77*, 3865–3868.

43. Kresse, G.; Furthmüller, J. Efficient Iterative Schemes for *Ab-Initio* Total-Energy Calculations Using a Plane-Wave Basis Set. *Phys. Rev. B* **1996**, *54*, 11169–11186.

44. Kresse, G.; Hafner, J. *Ab Initio* Molecular Dynamics for Liquid Metals. *Phys. Rev. B* **1993**, *47*, 558–561.